

Analysis of Bathymetry Accuracy Using Sentinel 2 Satellite on Different Characteristics Waters in Bali Island

Ni Nyoman Pujianiki ^{a,*}, Komang Gede Putra Airlangga ^b

^a Civil Engineering, Udayana University, Kampus Bukit Jimbaran, 80361, Bali, Indonesia

^b Master of Civil Engineering, Udayana University, Kampus Sudirman Denpasar, 80234, Bali, Indonesia

Corresponding author: *pujianiki@civil.unud.ac.id

Abstract— Bathymetry surveys today are often carried out using the echo-sounding method, but this method has disadvantages, such as requiring a lot of time and being quite expensive. Along with the development of technology, some alternative methods can be used to visualize bathymetry, such as remote sensing. Remote Sensing uses satellite imagery in the operation, while the technique to acquire bathymetry is called Satellite-Derived Bathymetry (SDB). This method uses an optical satellite with several color bands or multispectral images. In this research, a satellite used to map ocean depth is Sentinel-2. The SDB technique used in this research is the Lyzenga Algorithm. The Lyzenga algorithm uses multilinear logarithms in its operation and can be used using three optical image channels (blue, green, and red channels). Supported by the SDB algorithm, an analysis of research locations was carried out at several points in the waters of Bali Island due to the diversity of water characteristics such as sea depth and wave height. From several analysis results of different characteristic waters in Bali Island, We can see that many parameters impact the result of the Satellite to visualize bathymetry. The Satellite's optimal result for reading the bathymetry depth is approximately 30 meters. But in reality, some cases can interfere with the accuracy of Satellite visualizing bathymetry within this depth. Breaking waves, high water sedimentation, and some objects that could guide the Satellite to misread them as elevation.

Keywords— Bathymetry; remote sensing; sentinel-2; Bali Island; lyzenga algorithm.

Manuscript received 1 Mar. 2024; revised 10 Jul. 2024; accepted 3 Aug. 2024. Date of publication 31 Aug. 2024.
IJASEIT is licensed under a Creative Commons Attribution-Share Alike 4.0 International License.



I. INTRODUCTION

Bathymetric surveys today are often carried out using the echo sounding method, either single beam or multibeam [1]–[3]. This method has disadvantages, including requiring a lot of time and being expensive [4], [5]. The scope that can be surveyed is also limited because ships carrying echosounders cannot reach shallow-depth coasts. Due to these limitations, looking for an alternative method to obtain results with a broader range but in a more efficient time is necessary. Along with the development of technology, some alternative methods can be used to map the sea depth, such as Remote Sensing [6], [7]. This method uses the help of satellite or UAV imagery, which consists of several color bands called multispectral. Several previous studies in Remote Sensing have been carried out, such as to examine changes in coastlines [8]–[10], rip current investigations [11], and bathymetry derivation [12].

Remote Sensing using radar satellites or Synthetic Aperture Radar (SAR) cannot be used to map ocean depths,

even though radar satellites are often used to map land topography. This is due to the inability of the SAR sensor to penetrate the water surface. Waves from the SAR sensor will be reflected when they hit the water surface. Therefore, the satellite is an optical satellite type due to these limitations. Optical satellites generally consist of several color bands that image objects on the Earth's surface [13]. Each optical satellite has a different number and wave bands. This typically depends on the function and institution that launched the satellite. For years, optical satellite data has been used by many different researchers with the evolving algorithms [14]. In this research, the optical satellite used is Sentinel-2. Sentinel-2 launched by the European Union Space Agency (ESA), which Copernicus Sentinel-2A and Sentinel-2B optical satellites have been fully operating since June 2017 [15]. Sentinel-2 imagery has a reasonably high spatial resolution, i.e., 10 meters, and is available for free and in real-time on the internet to the public [16].

The method for mapping ocean depths using multispectral satellites is often called Satellite-Derived Bathymetry (SDB)

[14], [17]–[19]. SDB is a technique in remote sensing that utilizes satellite image data to obtain water-depth information [20]–[22]. The SDB technique, the Lyzenga Algorithm, was used in this research. The Lyzenga algorithm uses multilinear logarithms in its operation and can be used using three optical image channels (blue, green, and red channels). The coefficients resulting from multilinear regression are the components of an equation. This equation is applied to the channels from the previous Lyzenga algorithm processing. This process is also often called depth extraction (vertical referencing). This process aims to change/convert pixel values into in situ depth values or relative depth into depth of field [23].

Supported by the SDB calculation algorithm, an analysis has been carried out on several research locations in some waters of Bali Province. Due to the diversity of water characteristics ranging from sea depth to wave size, we can find out how much influence the accuracy test results of satellite image data have on in situ or echosounder data.

II. MATERIALS AND METHODS

A. Materials

The data used in this research comes from satellite data and in situ bathymetric data from an echosounder's survey.

1) *Satellite Data*: Satellite data using optical satellite Sentinel-2 Level-2A from the Copernicus Data Space Ecosystem [24]. The data from satellite images has a different time from the data from in situ measurements using an echosounder. This is because, during the survey, clouds could cover the image captured by the satellite. So, for the satellite image data used in this research, the time closest to the time of the survey was searched, where the selected image must be free from cloud cover. This will cause bias in the bathymetric data when carrying out surveys with echo sounders. Because at different times, the water level has different heights. So, to equalize the perception of bathymetric data from echosounder measurements with satellite imagery, adjustments have been made in the form of tidal corrections. Tidal correction is carried out using the admiralty method to determine the height of the water level at the time the satellite image was captured.

2) *In-situ data*: In situ data were obtained using a single-beam echosounder at the research location. The bathymetric data obtained was then processed, and tidal corrections were carried out. After being corrected, an accuracy test was carried out using the results of the bathymetric (SDB) derivation from satellite images.

- *Sangsit Port*. Sangsit Harbor is in Sangsit Village, Sawan District, Buleleng Regency. Bathymetry-sounding data using an echosounder was carried out at this location on November 1, 2020. The location and bathymetric mapping route at Sangsit Port can be seen in the following image.



Fig. 1 Location and bathymetric path of Sangsit Port

- *Gunaksa Port*: Gunaksa Harbor is located in Gunaksa Village, Dawan District, Klungkung Regency. Bathymetric sounding data using an echo sounder at this location was collected on April 16, 2021. The location and bathymetric mapping route at Gunaksa Port can be seen in the following image.



Fig. 2 Location and bathymetric path of Gunaksa Port

- *Serangan Port*: Serangan Port is located in Serangan Village, South Denpasar District, Denpasar City. Bathymetric sounding data using an echo sounder at this location was carried out on June 7, 2021. The location and route for bathymetric mapping at Serangan Port can be seen in the following image.



Fig. 3 Location and bathymetric path of Serangan Port

B. Methods

Some methods were used in this research to achieve the results for discussion.

1) Image Pre-Processing and Correction

Before Sentinel-2 data can be used to analyze, it is necessary to do Image Pre-Processing and Correction

- *Resampling*. Sentinel-2 has a different spatial resolution for each band. Spatial resolution can be equated with the upscaling and six downscaling methods or what is usually called the resampling process. The most commonly used method for re-scaling pixel resolution is resampling using the nearest neighbor method [25].
- *Subset*. The subset needs to crop out the unnecessary area to focus the image dataset's area only on the research location.
- *Normalized Difference Water Index (NDWI)*. The NDWI (Normalized Difference Water Index) algorithm separates land and sea in images. This algorithm utilizes blue and near-infrared reflections to show an area's level of wetness [12]. A modified version of NDWI was proposed by [13], replacing the NIR band with the shortwave infrared (SWIR) band to eliminate noise from accumulation in coastal areas. The application of the NDWI algorithm is as follows.

$$NDWI = \frac{Green-SWIR1}{Green+SWIR1} \quad (1)$$

- *Masking.* After successfully carrying out the NDWI algorithm, the next step is eliminating the land parts. Masking is carried out to cover land areas by creating a new layer [26]. We can focus the observation only on sea parts.
- *Sun Glint Correction.* The results of the sun glint correction succeeded in reducing the effect of sunlight reflection on the surface, which causes light bias so that the quality of the appearance and digital number of the corrected image is better than the image before the correction [27]. A sun glint effect removal algorithm was developed [28] Which was refined by [29].

$$R'_i = R_i - b_i(R_{NIR} - min_{NIR}) \quad (2)$$

2) Lyzenga Algorithm

The Lyzenga algorithm was discovered and developed by [30] and continues to experience development through a series of scientific research in [31], [32], [33], [34] and [19]. The Lyzenga algorithm, often called Depth Invariant Index (DII), is an algorithm applied to images for water column correction [35]. The principle of this algorithm is to use a combination of visible light channels of satellite images. This technique was previously described to determine the condition of the bottom of the waters using Landsat images based on the linear function of bottom reflectance in the waters and the exponential function of the depth of water [36]. The following is equation (3), which explains the Lyzenga algorithm.

$$Z = a_0 + \sum_{i=1}^N a_i \ln (R(\lambda_i) - R_{\infty}(\lambda_i)) \quad (3)$$

3) Multilinear Regression

In the principle of shallow sea depth extraction using satellite imagery, there are four main components: atmospheric scattering, surface reflection, in-water volume scattering, and bottom reflection. The Bottom reflection component is the main component used as a value in producing sea depth. At the same time, the other three elements are residual or noise components that need to be removed or searched for values to correct the spectral value of the image received by the sensing satellite. Estimating sea depth using satellite imagery can be carried out using various models. The SDB model, which is very simple and frequently used, is a multiple linear regression analysis. The general equation is

$$y = b_1x_1 + b_2x_2 + b_3x_3 + \dots + b_ix_i + a \quad (4)$$

4) Accuracy Test

RMSE is a forecasting technique used to evaluate a model's accuracy level. RMSE is the average value of the sum of squared errors. It can also express the size of the error produced by an estimation model, a bathymetry comparison between satellite and in situ models. RMSE can be calculated as follows:

$$RMSE = \sqrt{\frac{\sum_{t=1}^n (At-Ft)^2}{n}} \quad (5)$$

III. RESULT AND DISCUSSION

Based on methods from image pre-processing and applying the algorithm to every location. The following results were obtained.

A. Sangsit Port

Sentinel-2 Level-2A data product used for Sangsit Port was recorded on August 25, 2021, 02:16 UTC. According to admiralty calculations, the water level is at +1.30 m, while the LAT (Lowest Astronomical Tide) is at +0.40 m. Therefore, a correction was made between the height of the satellite data and the in-situ data by 0.90 m for calibration. From the results of processing satellite data and applying the Lyzenga Algorithm to Sangsit Port, the accuracy using multilinear regression is shown in Table 1.

TABLE I
ACCURACY VALUE WITH MULTILINEAR REGRESSION OF LYZENGA ALGORITHM AT SANGSIT PORT

Variable	Correlation Value	Equation	R ²	RMSE
x_i (B1/B2)	0.769	$y=294.13x-252.43$	0.346	28.615
x_j (B1/B3)	0.457	$y=161.51x-315.49$	0.445	26.365
x_k (B2/B3)	0.547	$y=189.59x-279.87$	0.358	28.361
$x_i+x_j+x_k$		$y=-965.57x_i+1108.32x_j-776.46x_k-125.51$	0.451	26.247

From the multilinear regression table and the equation above, the next step is to rewrite the equation to SNAP software to get the relative depth value. Figure 4 shows a graph comparing the depth using the Lyzenga algorithm to in situ.

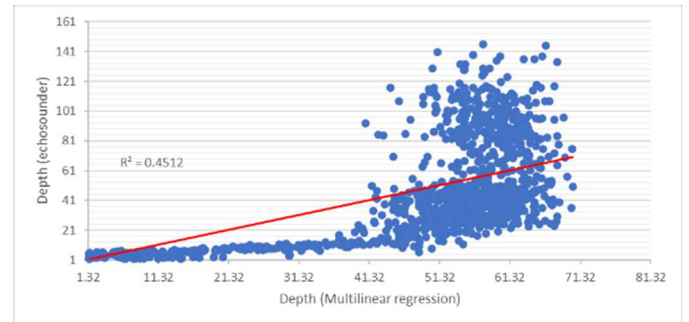


Fig. 4 Lyzenga Algorithm Depth Graph compared to in situ at Sangsit Port

From the results of processing at Sangsit Port. The Lyzenga algorithm has an accuracy of coefficient of determination / R² at 0.451. Meanwhile, the level of error / RMSE was at 26,224. The comparison of the bathymetric map between in situ and the Lyzenga algorithm is shown in Figure 5.

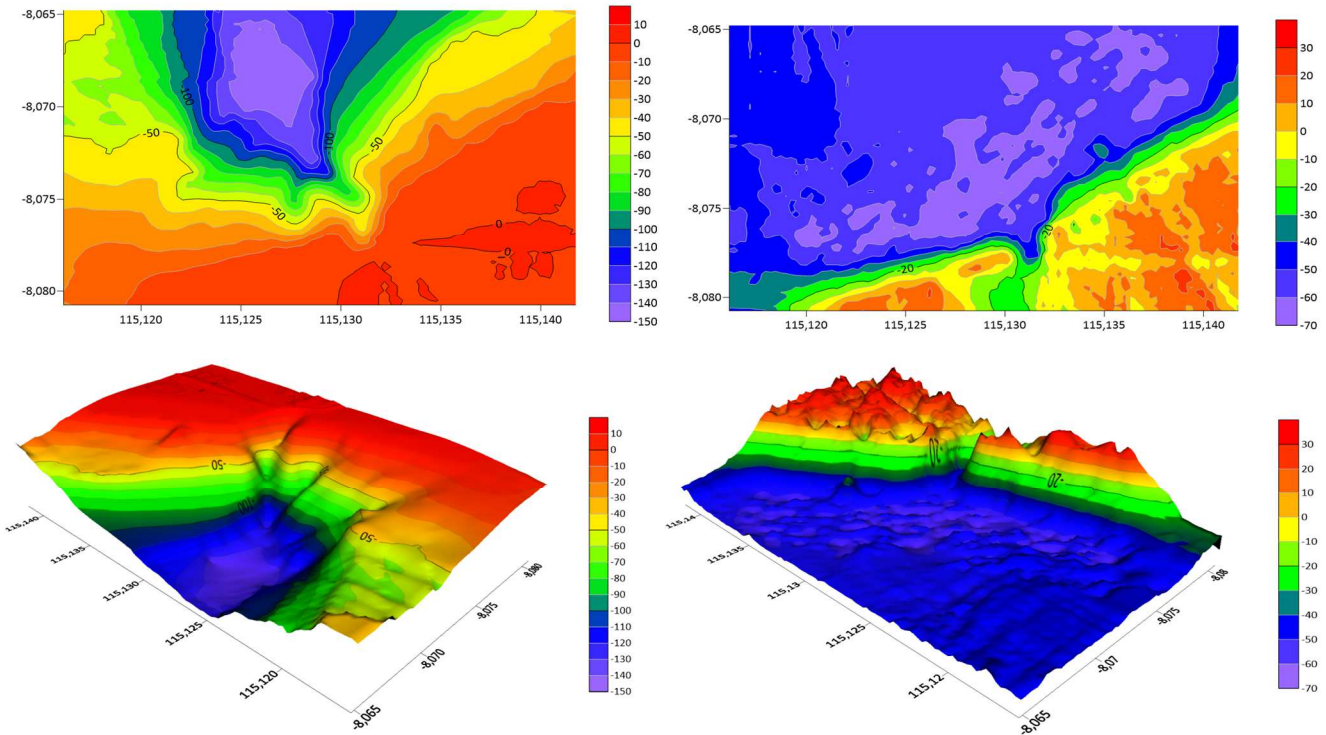


Fig. 5 2D and 3D Visualization of Bathymetry in-situ (left) and Lyzenga algorithm (right) at Sangsit Port

From the bathymetric map plotting between the in-situ data and Lyzenga algorithm, there are differences can be seen in depth levels visualization where the Lyzenga algorithm were only able to penetrate depth for up to 70 m instead of in situ data at 150 m. Analysis was carried out to prove that depth influences the accuracy results of satellite images in

visualizing bathymetry by limiting depth data to 20 m. This depth is based on previous research that bathymetry using remote sensing obtained good results up to 20 m [37], [38]. The results of bathymetry visualization after depth limitation are shown in Figure 6.

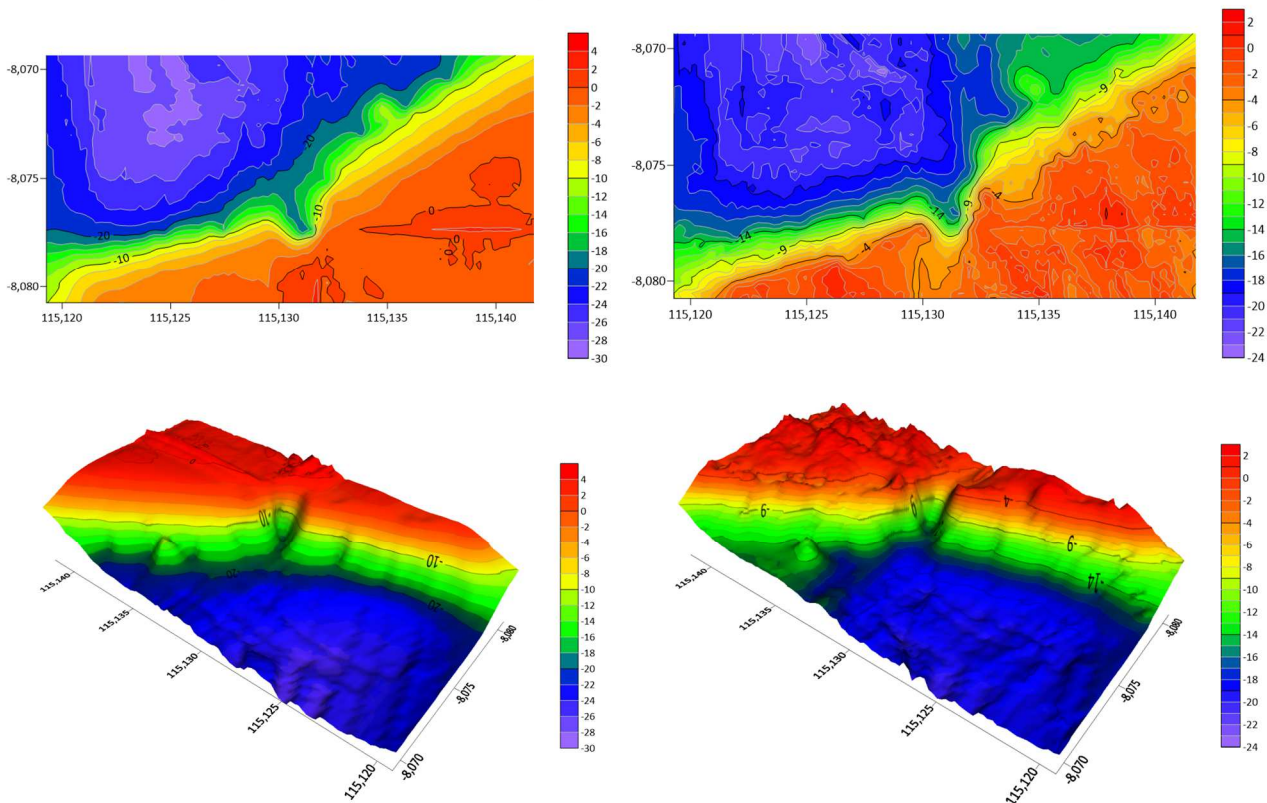


Fig. 6 2D and 3D Visualization of Bathymetry in-situ (left) and Lyzenga algorithm (right) at Sangsit Port after trimming depth data

After trimming the data and limiting the depth to 20 m, it was proven that the bathymetric visualization was better than the previous. Furthermore, to determine the level of accuracy, a regression test was carried out once again within this data. The correlation depth after limitation is shown in Figure 7.

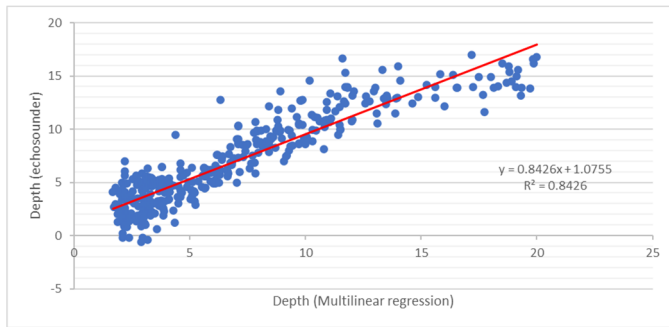


Fig. 7 Lyzenga Algorithm Depth Graph after depth limitation at Sangsit Port

From the data trimming that has been carried out, a better accuracy value is obtained with a coefficient of determination (R^2) of 0.844 with a RMSE of 1.826. This proves that depth influences the accuracy results of satellite images in visual bathymetry.

B. Gunaksa Port

Sentinel-2 Level-2A data product used for Gunaksa Port was recorded on June 6, 2022, 02.16 UTC. According to admiralty calculations, the water level is at +0.70 m, while the LAT (Lowest Astronomical Tide) is at +0.50 m. Therefore, a correction was made between the height of the satellite data and the in-situ data by 0.20 m for calibration. From the results of processing satellite data and applying the Lyzenga Algorithm to Gunaksa Port, the accuracy using multilinear regression is shown in Table 2.

TABLE II
ACCURACY VALUE WITH MULTILINEAR REGRESSION OF LYZENGA ALGORITHM AT GUNAKSA PORT

Variable	Correlation Value	Equation	R^2	RMSE
x_i (B1/B2)	0.863	$y = -78.80x + 84.15$	0.034	44.165
x_j (B1/B3)	0.683	$y = -46.66x + 103.31$	0.019	44.492
x_k (B2/B3)	0.804	$y = 5.70x + 37.30$	$3E-4$	44.924
$x_i + x_j + x_k$		$y = 11288.49x_i - 11406.5x_j + 9656.8x_k + 569.41$	0.495	31.942

From the table of multilinear regression and the equation above, the next step is to rewrite the equation to SNAP software to get the relative depth value. Figure 8 shows a graph comparing the depth using the Lyzenga algorithm to in situ.

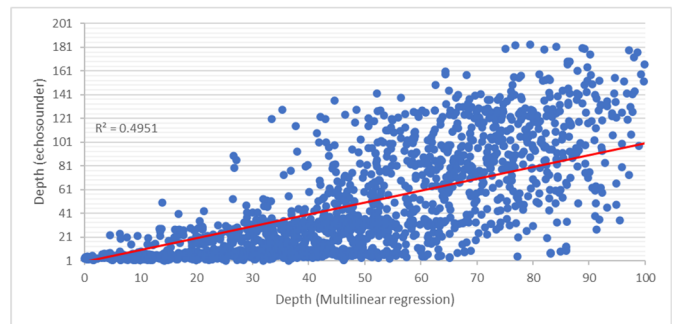


Fig. 8 Lyzenga Algorithm Depth Graph compared to in situ at Gunaksa Port

From the results of processing at Gunaksa Port. The Lyzenga algorithm has an accuracy of coefficient of determination / R^2 at 0.451. Meanwhile, the level of error / RMSE was at 31.942. The comparison of the bathymetric map between in situ and with the Lyzenga algorithm is shown in Figure 9.

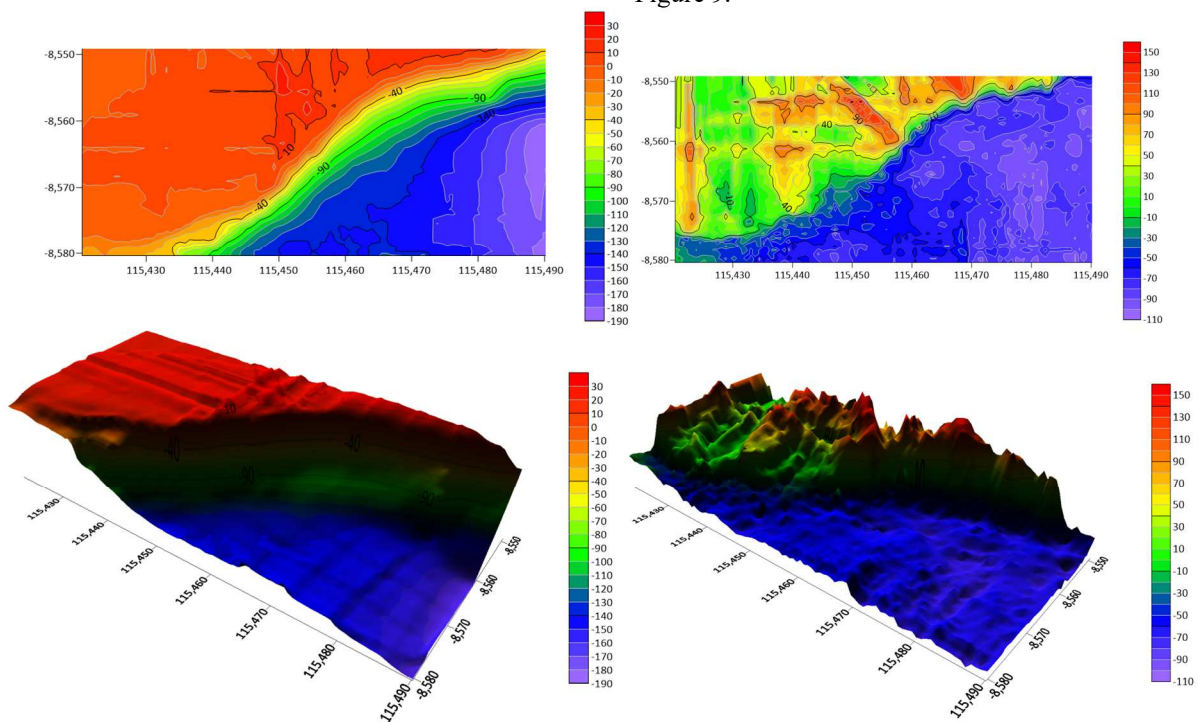


Fig. 9 2D and 3D Visualization of Bathymetry in-situ (left) and Lyzenga algorithm (right) at Gunaksa Port

From the bathymetric map plotting between the in-situ data and the Lyzenga algorithm, bathymetry with the Lyzenga algorithm has poor results because of the difference in depth limit. In situ, depth has a maximum depth of up to 190 meters, whereas, in the Lyzenga algorithm, it only reaches 110 m. This result is similar to the previous case at Sangsit Port, where the SDB could not reach waters with high depth. Gunaksa Port is one of the waters with deep water characteristics. Therefore, it is necessary to carry out accuracy tests again by trimming data on waters for up to 30 meters. The results of these data trimmings are shown in Figure 10.

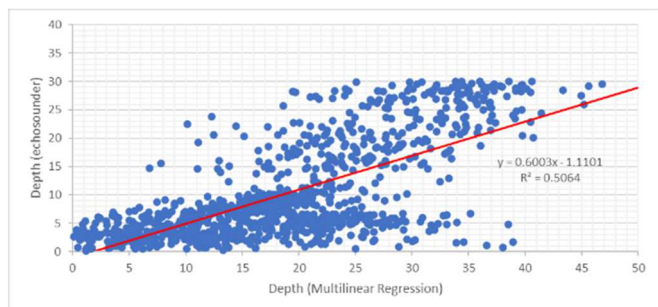


Fig. 10 Lyzenga Algorithm Depth Graph after depth trimming at Gunaksa Port

After trimming the depth data for up to 30 meters, there is an increase in the accuracy value from the previous data, with the new R^2 value of 0.506. This proves that depth can influence the accuracy of measuring bathymetry. But this still needs analysis. Based on the previous 3D bathymetry visualization with the Lyzenga algorithm, we can see the image of breaking waves in shallow areas. Back to the satellite image, the breaking wave area at Gunaksa Port is shown with red points, which are shown in Figure 11.

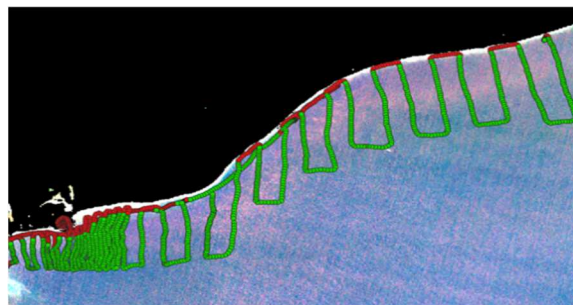


Fig. 11 Location of breaking waves at Gunaksa Port

After eliminating data suspected to be the location of breaking waves, the depth data obtained starts at an elevation of 4.7 m. After removing the data on the breaking waves, an accuracy test was carried out again, and the accuracy of the coefficient of determination / R^2 results is shown in Figure 12.

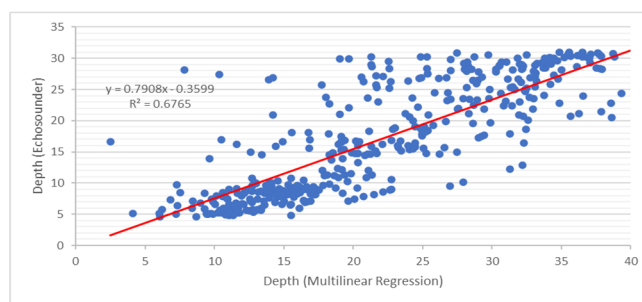


Fig. 12 Lyzenga Algorithm Depth Graph after trimming breaking waves data and depth limitation at Gunaksa Port

The result of bathymetry visualization after trimming breaking waves data and depth limitation at Gunaksa Port are shown in Figure 13

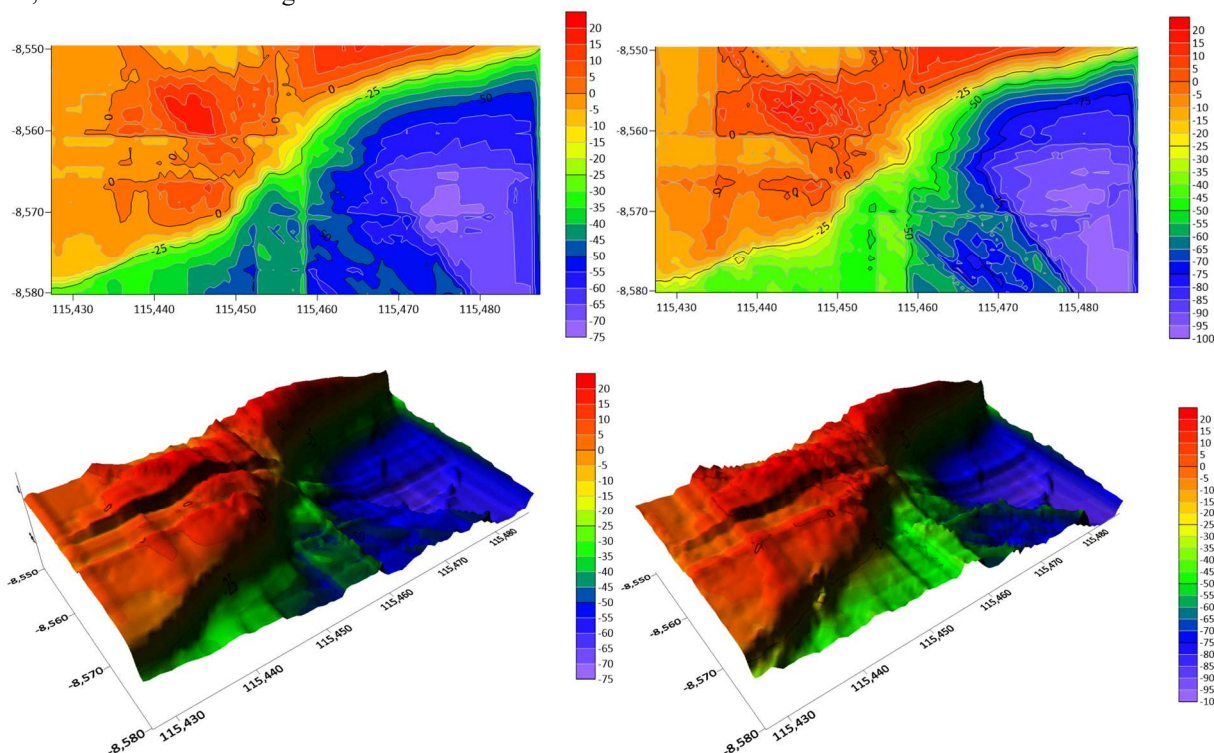


Fig. 13 2D and 3D Visualization of Bathymetry in-situ (left) and Lyzenga algorithm (right) at Gunaksa Port after trimming breaking waves and depth data

From the data trimming that has been carried out, a better accuracy value is obtained with an accuracy value coefficient of determination (R^2) of 0.677 with an RMSE of 5.060. This proves that apart from depth, the presence of breaking waves in the waters also influences the results of the accuracy of satellite images in visualizing bathymetry. It can be concluded that the satellite image band readings become inaccurate due to light refraction.

C. Serangan Port

Sentinel-2 Level-2A data product used for Serangan Port was recorded on June 6, 2022, 02.16 UTC. According to admiralty calculations, the water level is at +1.10 m, while the LAT (Lowest Astronomical Tide) is at +0.30 m.

TABLE III
ACCURACY VALUE WITH MULTILINEAR REGRESSION OF LYZENGA ALGORITHM AT SERANGAN PORT

Variable	Correlation Value	Equation	R^2	RMS E
x_i (B1/B2)	0.769	$y=2.37x+3.29$	0.059	3.504
x_j (B1/B3)	0.457	$y=3.20x+4.29$	0.151	3.329
x_k (B2/B3)	0.547	$y=8.50x+5.04$	0.184	3.264
$x_i+x_j+x_k$		$y=-106.19x_i+107.04x_j-95.27x_k+17.13$	0.311	3.000

Therefore, a correction was made between the height of the satellite data and the in-situ data by 0.80 m for calibration.

From the results of processing satellite data and applying the Lyzena Algorithm to Serangan Port, the accuracy using multilinear regression is shown in Table 3.

From the table of multilinear regression and equation above, the next step is rewriting the equation to SNAP software to get the relative depth value. The graph of comparison between the depth using the Lyzena algorithm and in situ is shown in Figure 14.

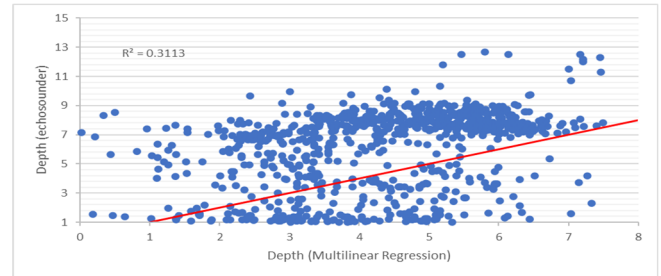


Fig. 14 Lyzena Algorithm Depth Graph compared to in situ at Serangan Port

From the results of processing at Serangan Port. The Lyzena algorithm has an accuracy of coefficient of determination / R^2 at 0.311. Meanwhile, the level of error / RMSE is at 3,000. The comparison of the bathymetric map between in situ and with the Lyzena algorithm is shown in Figure 15.

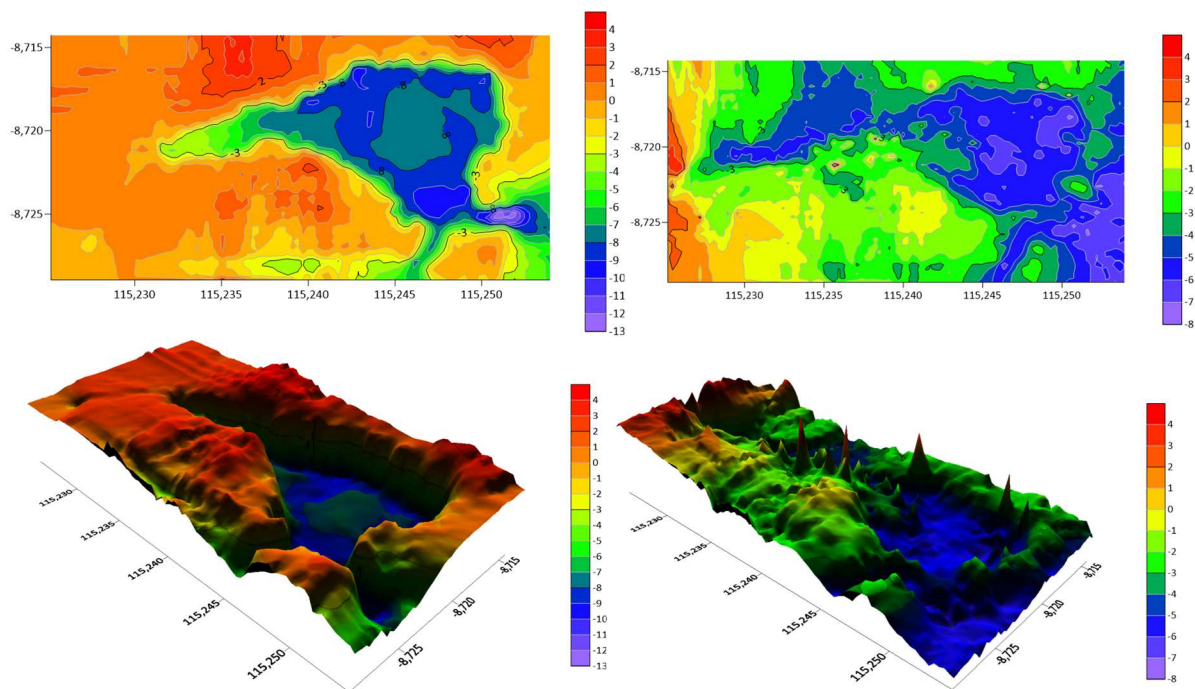


Fig. 15 2D and 3D Visualization of Bathymetry in-situ (left) and Lyzena Algorithm (right) at Serangan Port

Serangan Port is a natural Port, meaning it does not need coastal protection to create calm water conditions. Besides that, Serangan Port also has a relatively shallow bathymetric profile compared to other waters. Even with this good condition. Serangan Port has a bad accuracy in reading bathymetry using satellites. From the bathymetric map plotting between the in-situ data and the Lyzena algorithm, the difference can be seen in the port basin area, where this location can't be mapped perfectly at Lyzena visualization.

This could happen because, at the time when the image was captured by satellite, there were object interferences in the port basin, which resulted in misinformation about the separation between land and water. It can be seen from the visualization of 3D bathymetry images using the Lyzena algorithm where objects such as coral rise upwards. These objects were ships parked in the port basin area when the image was captured, while these objects did not exist at the time when the recording used an echosounder. By this

condition, an analysis has been made by tried eliminating several echosounder recording points in the area. Points that have been deleted are shown in red color in Figure 16.



Fig. 16 Object interferences location of parked ships in Serangan Port

The accuracy values are shown in Figure 17, which shows the data elimination results from removing object interferences of parked ships in the basin port area at Serangan Port.

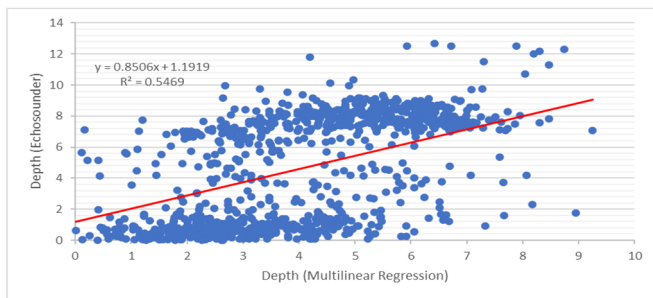


Fig. 17 Depth Graph after trimming the object interferences with the Lyzenga Algorithm at Serangan Port

From the results of the graph in Figure 17, it can be seen that accuracy value has slightly improved due to removing some points that contain object interferences of parked ships. However, these results still require re-analysis of objects, which can still be why the accuracy value is low. Analysis has been carried out by calculating the high % of error, above 100% for each point. Several points have been analyzed, then marked and extracted again according to the coordinates to make

identifying areas or locations with high errors easier. These points can be shown in yellow color as shown in Figure 18.

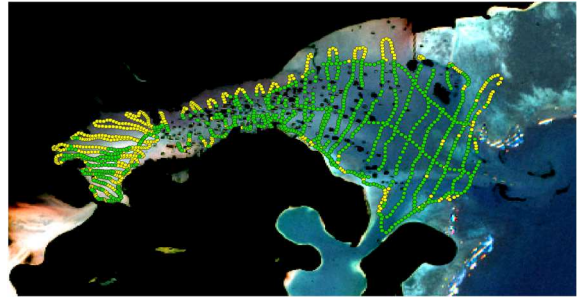


Fig. 18 The location which have high error at Serangan Port

Based on the map from the satellite image in Figure 15, it can be identified that locations with high errors are predominantly found in waters that have a slightly brownish color. These waters can be assumed because of a high level of sedimentation. This can be confirmed by the profile of Serangan Water, which has a high amount of total suspended solid (TSS) in the water near the mangrove forest area on the port's north side. Several known points have been tried to be eliminated, and the results obtained are shown in Figure 19.

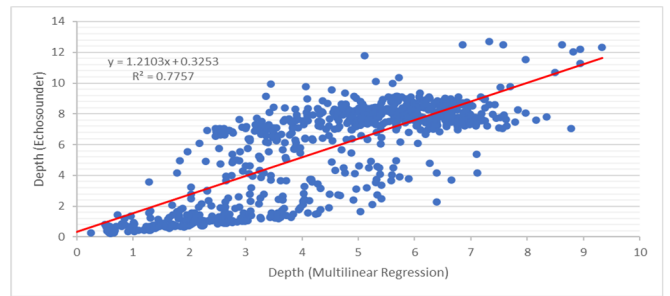


Fig. 19 Lyzenga Algorithm Depth Graph after elimination of high-water sedimentation points at Serangan Port

Figure 20 shows the result of bathymetry visualization after eliminating interference objects, such as parked ships and high-water sedimentation points at Serangan Port.

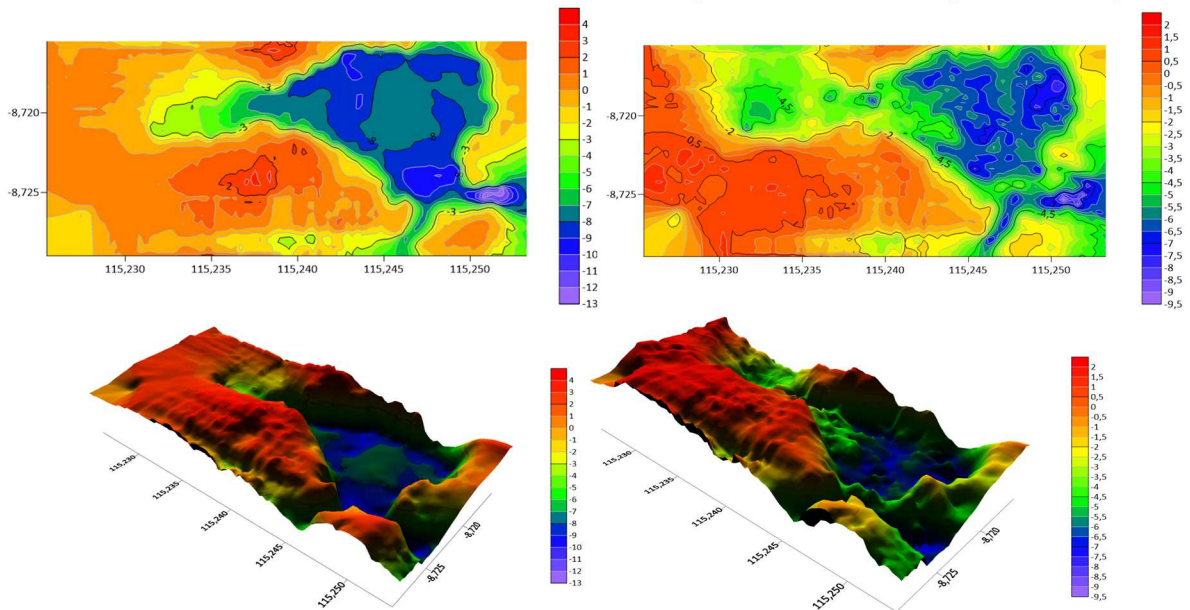


Fig. 20 2D and 3D Visualization of Bathymetry in-situ (left) and Lyzenga Algorithm (right) at Serangan Port after elimination interference object of parked ships and high-water sedimentation points at Serangan Port

From data elimination carried out on the interference object of parked ships and high-water sedimentation points, a better accuracy value is obtained with an accuracy value coefficient of determination (R^2) of 0.775 with RMSE of 1.730. These results can confirm that apart from the interference objects of ships that parked at the basin port area at Serangan Harbor, high-level sedimentation in the water also influences the level of accuracy in visualizing bathymetry using satellite [39]. It can be confirmed from the test carried out in the laboratory at this location that this area has a high amount of TSS. Sedimentation conditions in a water area can be determined by how extensive the range of suspended solid material is in that area [40]. Generally, the SDB model is strongly influenced by the type of sensor, water quality, and other environmental conditions. It also stated in [41] about factors of water column complexity, such as the heterogeneity of water quality and sedimentation affect the accuracy of estimating the water depth.

IV. CONCLUSION

Several results of analyzing bathymetry using Sentinel-2 Imagery in different characteristic waters on Bali Island. We can see that many parameters impact the result of the Satellite to visualize bathymetry. The Satellite's optimal result in reading the bathymetry depth is approximately 30 meters. However, within this depth, some cases can interfere with the accuracy of satellite visualizing bathymetry. Breaking waves, high water sedimentation, and some objects that can guide the Satellite to misread them as elevation, such as ships.

NOMENCLATURE

Sun Glint Correction

R'_i	value of i channel after reduction
R_i	initial value of i channel
b_i	the regression of slope
R_{NIR}	channel value
min_{NIR}	minimum value of NIR channel

Lyzenga Algorithm

Z	water depth
a_i	constant coefficient, ($i=0,1,\dots,n$) n is number of spectrum bands
$R(\lambda_i)$	Reflectance after atmospheric correction for λ_i spectrum band
$R_x(\lambda_i)$	Average deep of sea reflectance in λ_i spectrum band

Multilinear Regression

y	dependent variable
x	independent variable
a	intercept, (y when $x=0$)
b	slope, the average change in y relative to x

Accuracy Test

At	Depth estimation value of image
Ft	in situ measurement value
N	The number of depth points used in model validation

ACKNOWLEDGMENT

The authors thank Research and Community Service (LPPM UNUD) for funding this research on the INSPIRE program.

REFERENCES

- [1] Z. Li et al., "Exploring modern bathymetry: A comprehensive review of data acquisition devices, model accuracy, and interpolation techniques for enhanced underwater mapping," *Frontiers in Marine Science*, vol. 10, May 2023, doi: 10.3389/fmars.2023.1178845.
- [2] H. M. Dierssen and A. E. Theberge, "Bathymetry: Assessment," *Coastal and Marine Environments*, pp. 175–184, May 2020, doi:10.1201/9780429441004-19.
- [3] I. O. Ferreira, L. C. de Andrade, V. G. Teixeira, and F. C. M. Santos, "State of art of bathymetric surveys," *Boletim de Ciências Geodésicas*, vol. 28, no. 1, 2022, doi: 10.1590/s1982-21702022000100002.
- [4] F. Tsukada, T. Shimozono, and Y. Matsuba, "UAV-based mapping of nearshore bathymetry over broad areas," *Coastal Engineering Journal*, vol. 62, no. 2, pp. 285–298, Apr. 2020, doi:10.1080/21664250.2020.1747766.
- [5] J. Wan and Y. Ma, "Shallow Water Bathymetry Mapping of Xinji Island Based on Multispectral Satellite Image using Deep Learning," *Journal of the Indian Society of Remote Sensing*, vol. 49, no. 9, pp. 2019–2032, Apr. 2021, doi: 10.1007/s12524-020-01255-9.
- [6] T. Kutser, J. Hedley, C. Giardino, C. Roelfsema, and V. E. Brando, "Remote sensing of shallow waters – A 50 year retrospective and future directions," *Remote Sensing of Environment*, vol. 240, p. 111619, Apr. 2020, doi: 10.1016/j.rse.2019.111619.
- [7] E. Vahtmäe and T. Kutser, "Mapping Bottom Type and Water Depth in Shallow Coastal Waters with Satellite Remote Sensing," *Journal of Coastal Research*, vol. 50, no. sp1, Jun. 2007, doi: 10.2112/jcr-si50-036.1.
- [8] N. N. Pujianiki, G. B. A. S. Widhi, I. N. G. Antara, I. G. R. M. Temaja, and T. Osawa, "Monitoring Coastline Changes Using Landsat Application in Batu Mejan Beach," *International Journal on Advanced Science, Engineering and Information Technology*, vol. 11, no. 2, pp. 738–745, Apr. 2021, doi: 10.18517/ijaseit.11.2.13162.
- [9] N. N. Pujianiki, I. N. Sudi Parwata, and T. Osawa, "A New Simple Procedure for Extracting Coastline from SAR Image Based on Low Pass Filter and Edge Detection Algorithm," *Lontar Komputer : Jurnal Ilmiah Teknologi Informasi*, vol. 12, no. 3, p. 175, Nov. 2021, doi:10.24843/lkjiti.2021.v12.i03.p05.
- [10] N. N. Pujianiki, "Coastline changes monitoring induced by man-made structures using synthetic aperture radar: A new simple approach," *IOP Conference Series: Earth and Environmental Science*, vol. 1117, no. 1, p. 012041, Dec. 2022, doi: 10.1088/1755-1315/1117/1/012041.
- [11] P. NN, A. ING, T. IGRM, P. IGDY, and O. T, "Application of UAV in Rip Current Investigations," *International Journal on Advanced Science, Engineering and Information Technology*, vol. 10, no. 6, pp. 2337–2343, Dec. 2020, doi: 10.18517/ijaseit.10.6.12620.
- [12] M. D. M. Manessa et al., "Preliminary Result of Drone UAV Derived Multispectral Bathymetry in Coral Reef Ecosystem: A Case Study of Pemuteran Beach," *International Journal on Advanced Science, Engineering and Information Technology*, vol. 12, no. 4, p. 1512, Jul. 2022, doi: 10.18517/ijaseit.12.4.16107.
- [13] V. Khokhlov, V. Lukin, and S. Khokhlov, "Modelling full-colour images of Earth: simulation of radiation brightness field of Earth's atmosphere and underlying surface," *Annals of GIS*, vol. 29, no. 1, pp. 143–161, Apr. 2022, doi: 10.1080/19475683.2022.2064911.
- [14] M. Ashphaq, P. K. Srivastava, and D. Mitra, "Review of near-shore satellite derived bathymetry: Classification and account of five decades of coastal bathymetry research," *Journal of Ocean Engineering and Science*, vol. 6, no. 4, pp. 340–359, Dec. 2021, doi: 10.1016/j.joes.2021.02.006.
- [15] B. Pflug et al., "Next updates of atmospheric correction processor Sen2Cor," *Image and Signal Processing for Remote Sensing XXVI*, Sep. 2020, doi: 10.1117/12.2574035.
- [16] Syam'ani, "Potensi Pemanfaatan Teknologi Citra Esa Sentinel-2 Msi Untuk Pemantauan Kualitas Air," *Pros. Semin. Nas. Lingkungan. Lahan Basah*, vol. 6, no. April, pp. 1–8, 2021.
- [17] T. Duplančić Leder, M. Baučić, N. Leder, and F. Gilić, "Optical Satellite-Derived Bathymetry: An Overview and WoS and Scopus Bibliometric Analysis," *Remote Sensing*, vol. 15, no. 5, p. 1294, Feb. 2023, doi: 10.3390/rs15051294.

- [18] M. Al Najar, G. Thoumyre, E. W. J. Bergsma, R. Almar, R. Benschila, and D. G. Wilson, "Satellite derived bathymetry using deep learning," *Machine Learning*, vol. 112, no. 4, pp. 1107–1130, Jul. 2021, doi:10.1007/s10994-021-05977-w.
- [19] G. Casal, P. Harris, X. Monteys, J. Hedley, C. Cahalane, and T. McCarthy, "Understanding satellite-derived bathymetry using Sentinel 2 imagery and spatial prediction models," *GIScience & Remote Sensing*, vol. 57, no. 3, pp. 271–286, Nov. 2019, doi:10.1080/15481603.2019.1685198.
- [20] A. Knudby and G. Richardson, "Incorporation of neighborhood information improves performance of SDB models," *Remote Sensing Applications: Society and Environment*, vol. 32, p. 101033, Nov. 2023, doi:10.1016/j.rsase.2023.101033.
- [21] M. Niroumand-Jadidi, F. Bovolo, and L. Bruzzone, "SMART-SDB: Sample-specific multiple band ratio technique for satellite-derived bathymetry," *Remote Sensing of Environment*, vol. 251, p. 112091, Dec. 2020, doi:10.1016/j.rse.2020.112091.
- [22] M. U. Nuha, A. Basith, and W. Asriningrum, "Optimalisasi Parameter Analisis Ekstraksi Kedalaman Laut dengan Citra Satelit Resolusi Tinggi Pada Zona Laut Dangkal," Universitas Gadjah Mada, 2019.
- [23] S. Aji, A. Sukmono, and F. J. Amarrohman, "Analisis Pemanfaatan Satellite Derived Bathymetry Citra Sentinel-2A Dengan Menggunakan Algoritma Lyzenga Dan Stumpf (Studi Kasus : Perairan Pelabuhan Malahayati, Provinsi Aceh)," *Jurnal Geodesi Undip*, vol. 10, no. 1, pp. 68–77, Dec. 2020, doi:10.14710/jgundip.2021.29624.
- [24] A. T. Monteiro et al., "Remote sensing of vegetation and soil moisture content in Atlantic humid mountains with Sentinel-1 and 2 satellite sensor data," *Ecological Indicators*, vol. 163, p. 112123, Jun. 2024, doi:10.1016/j.ecolind.2024.112123.
- [25] A. Octaviana, Y. Prasetyo, and F. J. Amarrohman, "Analisis Perubahan Nilai Total Suspended Solid Tahun 2016 Dan 2019 Menggunakan Citra Sentinel 2a (Studi Kasus : Banjir Kanal Timur, Semarang)," *Jurnal Geodesi Undip*, vol. 9, no. 2, pp. 167–176, Apr. 2020, doi:10.14710/jgundip.2020.27178.
- [26] S. N. Syaiful, M. Helmi, S. Widada, R. Widiaratih, P. Subardjo, and A. A. D. Suryoputro, "Analisis Digital Citra Satelit Worldview-2 untuk Ekstraksi Kedalaman Perairan Laut di Sebagian Perairan Pulau Parang, Kepulauan Karimunjawa, Provinsi Jawa Tengah," *Indonesian Journal of Oceanography*, vol. 1, no. 1, pp. 36–43, Nov. 2019, doi:10.14710/ijoce.v1i1.6262.
- [27] W. Arifin, F. Febriandi, and T. Triyatno, "Pemetaan Kedalaman Perairan Danau Maninjau Dengan Algoritma Empirical Bathymetry Method Pada Citra Sentinel 2A," *El-Jughrafiyah*, vol. 1, no. 1, p. 29, Aug. 2021, doi:10.24014/jej.v1i1.14038.
- [28] E. J. Hochberg, S. Andrefouet, and M. R. Tyler, "Sea surface correction of high spatial resolution ikonos images to improve bottom mapping in near-shore environments," *IEEE Transactions on Geoscience and Remote Sensing*, vol. 41, no. 7, pp. 1724–1729, Jul. 2003, doi:10.1109/tgrs.2003.815408.
- [29] J. D. Hedley, A. R. Harborne, and P. J. Mumby, "Technical note: Simple and robust removal of sun glint for mapping shallow-water benthos," *International Journal of Remote Sensing*, vol. 26, no. 10, pp. 2107–2112, May 2005, doi:10.1080/01431160500034086.
- [30] D. R. Lyzenga, "Passive remote sensing techniques for mapping water depth and bottom features," *Applied Optics*, vol. 17, no. 3, p. 379, Feb. 1978, doi:10.1364/ao.17.000379.
- [31] E. C. Geyman and A. C. Maloof, "A Simple Method for Extracting Water Depth From Multispectral Satellite Imagery in Regions of Variable Bottom Type," *Earth and Space Science*, vol. 6, no. 3, pp. 527–537, Mar. 2019, doi:10.1029/2018ea000539.
- [32] L. Meliala, W. A. Wibowo, and J. Amalia, "Satellite Derived Bathymetry on Shallow Reef Platform: A Preliminary Result from Semak Daun, Seribu Islands, Java Sea, Indonesia," *KnE Engineering*, Dec. 2019, doi:10.18502/keg.v4i3.5849.
- [33] B. Gabr, M. Ahmed, and Y. Marmoush, "PlanetScope and Landsat 8 Imageries for Bathymetry Mapping," *Journal of Marine Science and Engineering*, vol. 8, no. 2, p. 143, Feb. 2020, doi:10.3390/jmse8020143.
- [34] K. T. Setiawan et al., "Utilization Of Semi-Analytical Methods For Determining Bathymetry Using High Resolution Satellite Images," *J. Penginderaan Jauh dan Pengolah. Data Citra Digit.*, vol. 18, no. 1, pp. 1–13, 2021.
- [35] A. Kartikasari, T. Pristiano, R. Hanintyo, E. E. Ampou, T. A. Wibawa, and B. B. Borneo, "Representative benthic habitat mapping on Lovina coral reefs in Northern Bali, Indonesia," *Biodiversitas Journal of Biological Diversity*, vol. 22, no. 11, Oct. 2021, doi:10.13057/biodiv/d221108.
- [36] F. Muhtar, A. Armijon, F. Murdapa, and R. Fadly, "Analisa Luasan Terumbu Karang Di Perairan Pulau Tegal Lampung Dengan Teknologi Penginderaan Jauh," *JGE (Jurnal Geofisika Eksplorasi)*, vol. 5, no. 2, pp. 141–153, Jan. 2020, doi:10.23960/jge.v5i2.29.
- [37] E. Evagorou, A. Argyriou, N. Papadopoulos, C. Mettas, G. Alexandrakakis, and D. Hadjimitsis, "Evaluation of Satellite-Derived Bathymetry from High and Medium-Resolution Sensors Using Empirical Methods," *Remote Sensing*, vol. 14, no. 3, p. 772, Feb. 2022, doi:10.3390/rs14030772.
- [38] H. Hossen, M. Khairy, S. Ghaly, A. Scozzari, A. Negm, and M. Elshabi, "Bathymetric and Capacity Relationships Based on Sentinel-3 Mission Data for Aswan High Dam Lake, Egypt," *Water*, vol. 14, no. 5, p. 711, Feb. 2022, doi:10.3390/w14050711.
- [39] C. Cahalane, A. Magee, X. Monteys, G. Casal, J. Hanafin, and P. Harris, "A comparison of Landsat 8, RapidEye and Pleiades products for improving empirical predictions of satellite-derived bathymetry," *Remote Sensing of Environment*, vol. 233, p. 111414, Nov. 2019, doi:10.1016/j.rse.2019.111414.
- [40] T. Prayoga and L. Sari Baru, "Analisis Penentuan Pembangunan Dermaga Berdasarkan Analisis Citra Sentinel 2a di Perairan Delta Wulan Kota Pesisir Demak," *Jurnal Indonesia Sosial Teknologi*, vol. 2, no. 11, pp. 2069–2081, Nov. 2021, doi:10.36418/jist.v2i11.276.
- [41] Z. Duan, S. Chu, L. Cheng, C. Ji, M. Li, and W. Shen, "Satellite-derived bathymetry using Landsat-8 and Sentinel-2A images: assessment of atmospheric correction algorithms and depth derivation models in shallow waters," *Optics Express*, vol. 30, no. 3, p. 3238, Jan. 2022, doi:10.1364/oe.444557.